Journal of Engineering Science and Technology
Vol. 2, No. 3 (2007) 218 - 225

ANALYSIS OF TURBULENT FLOW IN THE IMPELLER OF A CHEMICAL PUMP

MIN-GUAN YANG, DONG LIU*, XIANG DONG

School of Energy and Power Engineering, JiangSu University,
Zhenjiang, 212013, CHINA.
*Corresponding Author: liudong@ujs.edu.cn

Abstract

To study the phenomena of two-phase flow with salt crystallising in the chemical pump, the 3-D turbulent flow in the impeller of chemical pump was simulated at the condition of rinsing. The internal flow between the impellers of 1H65 chemical pump is investigated. Based on the Reynolds-averaging N-S equations and the standard k-ε two equations turbulent model, the simulations of turbulent flow between the impellers are performed using the flow computing software Fluent under different operating conditions. The calculation results are compared with the experimental data by particle image velocimetery (PIV). Based on the analysis of the calculated results of velocity and pressure profiles in the chemical pump and experimentally observed phenomenon of flow impact, secondary flow and recirculation, some design improvements are proposed, which give suggestions on the optimal design and internal two-phase flow study of the chemical pump.

Keywords: Chemical pump Impeller, Numerical simulation, PIV.

1. Introduction

The basic science problem of two-phase flow with salt crystallising in the centrifugal pump has always been a puzzle in the area of science and technology. Salt crystallising in the centrifugal pump is very common in paper making pulp and petrochemical manufacture. Because of the influence of viscosity and two-phase fluid with salt crystallizing, the flow in the impeller of centrifugal pump is very complex. Many researchers are always paying attention to the study of interior flow in centrifugal pump. The probe we used before can only measure one point. As the development of laser measurement technology, it is agreed that using PIV to study the interior flow of pump. There are many examples of application now.

Nomenclatures

b_2	Outlet breadth
D_2	Outer diameter
H	Pump head
n	Rotational speed
n_s	Specific speed
Q	Pump flux
Q_{opt}	Design flux of the pump
Δt	Pulse duration interval
u_x	Velocity in X direction
u_y	Velocity in Y direction
ΔX	Particle bit shift in the X direction
ΔY	Particle bit shift in the Y direction
z	Number of vanes

To reveal the real flow in impeller, the 3D turbulent flow in the impeller of centrifugal pump was studied at the condition of rinsing. Using simulation to conclude the distribution of velocity and pressure, and PIV to prove the interior flow in the impeller.

The CFD software FLUENT is used. Based on the Reynolds-averaging N-S equations and standard k-ε two equations turbulent model, the internal flow in the impeller with the work condition of 0.8 Q_{opt}, Q_{opt}, 1.2 Q_{opt} are calculated. Simultaneously the result of calculation is compared with PIV measurement, further understanding is obtained about the internal flow field in the impeller of chemical pump, and moreover, the research can provide reference for the two-phase flow research in the impeller.

2. The Numerical Simulation In The Impeller

2.1 Parameters of the impeller

The parameters of 3-D turbulent flow numerical simulated inside the impeller of the chemical pump are given in Table 1. The operating medium is water.

2.2 Calculated area and calculated grid

Nonconformal grids are adopted in this work. And during the process of plotting grids, inlet, outlet and wall are defined; the plotted grid result and the calculated area can be seen in Fig.1.

Table 1. Test Parameters.

Parameter	Value
Impeller outer diameter (D_2)	132 mm
Outlet breadth (b_2)	12 mm
Number of vanes (z)	6
Design flux (Q_{opt})	25 $m^3.h^{-1}$
Design head (H)	20 m
Rotating speed (n)	2890 rpm
Specific speed (n_s)	93

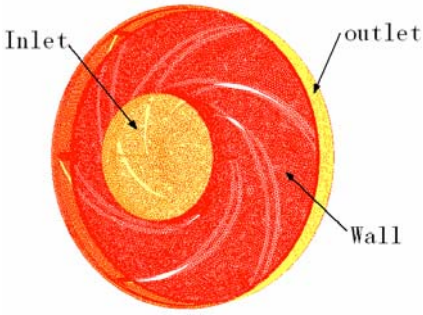

Figure 1 Diagrammatic Sketch of 3-D Model and Calculated Grid.

3 Experimental System and Principle

3.1 Experimental system

Figure 2 shows the experimental system. In order to meet the requirement of PIV system, we take the optimal design of chemical pump. The design flux of pump is 25 $m^3.h^{-1}$, design head is 20m, and the rotating speed is 2890 rpm. Both impeller and spiral casing back cover are made of glass, so the CCD camera could light the whole field in the impeller. A rectangle window was opened at the flank of spiral casing. The PIV system consists of a two-pulsed Nd-Yag laser, a CCD camera, a synchronizer and a data analysis system. The Laser with wavelength of 532nm has a frequency of 15 Hz. The output power of the laser is 120mJ/puls, which is sufficiently high for the experiment. The CCD camera was used to obtain digital images with 1248×1024 pixels, and can capture 3.75 pictures in one second. The particles used in these experiments are hollow glass particles with diameters of 8-10 micron.

The shaft encoder and frequency divider is used to deal with rotating flow. Shaft encode is fixed up on axes of motor. With every rotating of encoder, shaft encoder transmits 500 pulse signals which were divided by frequency divider to meet the speed collection of CCD. Figure 3 is the circuit of frequency divider.

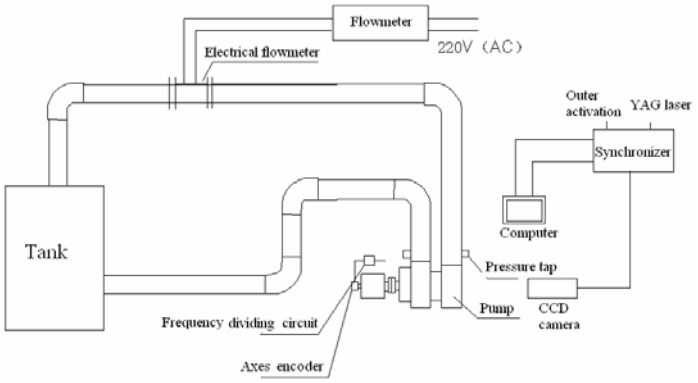

Fig. 2. Schematic of the Experimental System.

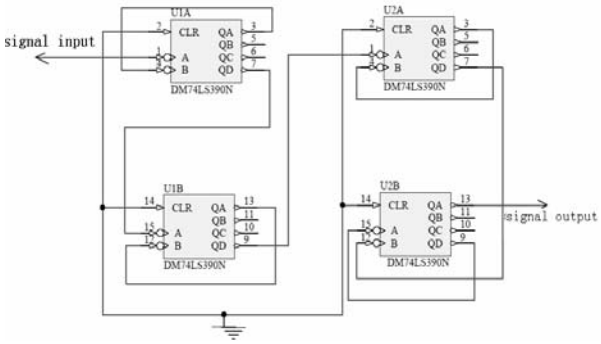

Fig.3. Circuit of Frequency Divider.

3.2 Basic principles of PIV

The basic principle of PIV is to measure the displacement of particles within a pulse duration interval Δt, in two directions, ΔX and ΔY, and then infer the velocity of the particle as follow:

$$u_x = \Delta X / \Delta t \tag{1}$$

$$u_y = \Delta Y / \Delta t \tag{2}$$

The principle is show in Fig 4. Due to the features of the tracer particles, particle's velocity is the same as the velocity of flow motion. The displacement of particles should be as small as possible to let $\Delta x / \Delta t$ close to particle's velocity. That's to say, within the time of Δt, the tracer of particles are almost lines and particle's velocity in the tracer is almost invariableness, which should be satisfied with a proper time of Δt.

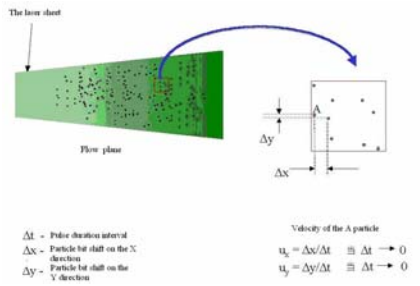

Fig. 4 Basic Principle of PIV.

4. Analysis of The Result of Calculations and Experiments

4.1 Relative speed distribution

Figure 5 shows the relative speed distribution for the work condition of $0.8Q_{opt}$, Q_{opt}, 1.2 Q_{opt}. It shows that, in the inlet and outlet of the impeller, the value of relative speed in the working face is same as that in the back face; while in the central section of the impeller, because of the affection of axial eddy, the value of relative speed in the back face is higher than that on the working face.

Comparing with the relative speed distribution of different work conditions, it is found that, as flux grows, the relative speed also grows continuously, and the area of low-speed is becoming smaller while the velocity gradient is becoming larger. The flux has no obvious influence to the direction of relative speed. Because of the high-speed revolution of the impeller, the rotating wall brings along the liquid particle, which makes the relative motion of liquid to the rotational movement.

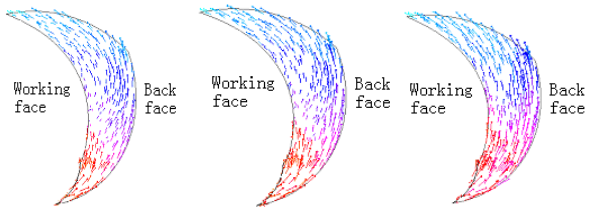

(a)The Small Flux (b) The Design Flux (c) The Big Flux

Fig.5. Relative Speed Distribution Obtained by the Numerical Simulation in Different Working Conditions.

Figure 6 shows the relative velocity distribution captured. The experimental results are comparative consistent with the calculated result. But as a result of the influence of the two below factors, the value of the relative speed is disaccord between the experiment and the calculation in certain areas.

1. Manufacturing inaccuracy of the impeller and the limit of the equipment condition.
2. Outlet velocity of the impeller gives an impact to the velocity in the extruding-room while the work condition is changed, which disturbs the internal flow of the impeller.

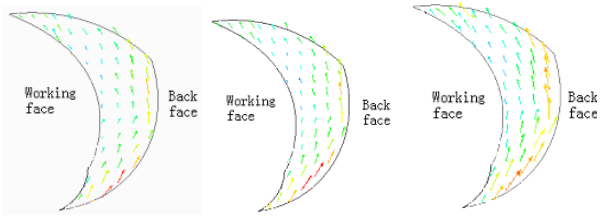

(a)The Small Flux (b) The Design Flux (c) The Big Flux

Fig.6. Relative Speed Distribution Obtained by the PIV in Different Working Condition.

4.2 Pressure Isoline Distribution

Figure 7 shows the pressure isoline in the impeller. Under the design work condition, the pressure distribution is more uniform. In the inlet and outlet of the impeller, the value of pressure in the working face is same as that in back face. While in the central section of the impeller, the value of pressure in the working face is higher than that in back face. With the increase of the flux, the outlet pressure becomes smaller. The value of the pressure gradually increases from the inlet to outlet and finally reaches the maximum in the outer brim of working face. Under the condition of small flux, the pressure isoline slants greatly between the vane working face and back face, and as flux increases, the gradient decreases gradually and in the flux of $1.2Q_{opt}$, the pressure isoline is almost parallel to the vane's surface, which means that with the process of the increasing flux and the decreasing pressure, the pressure between the vane working face and back face changes differently and the pressure decreases faster in back face than it is in working face.

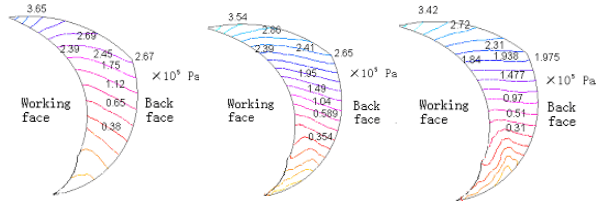

(a)The Small Flux (b) The Design Flux (c) The Big Flux

Fig.7. Pressure Isolines Obtained from the Numerical Simulation in Different Working Condition.

4.3 Analysis of secondary flow and loss of separation

Because of the diffusion of impeller channel, the boundary-layer separation happens easily. The fluid particle is subjected to the acting force right-about the pressure gradient because of the non-uniform pressure distribution. In the central section of the impeller, the acting force is in equilibrium with inertia force caused by the alteration of current velocity; While the current velocity is smaller in boundary-layer, inertia force can't equalize the acting force, which makes fluid particle in boundary-layer move to the direction right-about the pressure gradient, and the secondary flow arises with the flow direction vertical from the main flow and it also leads the loss of separation.

4.4 The loss of impaction while the work condition deviates the design condition

When the work condition of the pump deviates from design condition, the fluxion angle β_1 is different from the inlet allocation angle β_{b1}, and the flow separation in the surface of the vane and the loss of impaction in the inlet were captured in the process of PIV experiment; When the deviation became serious, many air bubbles and the vibration were found in the impeller which makes tracer particles wrongly reflect the statement of flow, as affects the result of the PIV experiment and influences the normal working of the pump as well.

4.5 The influence of the pump's performance when the vane is designed with forward attack angle

Figure 5 shows that the relative velocity decreases firstly and then increases in the working face, while the relative velocity in back face has the contrary variation. Because of this phenomenon, the area of vortex in the flow passage is generated. For the improvement of pump's cavitation, while using the method of forward attack angle, the setting angle will be larger which will narrow the area of vortex in the flow passage by liquid flow, enlarge the area of flow end plane, reduce the current velocity and improve the pump's cavitation performance as well.

5. Conclusions

The internal flow in the impeller of IH65 types chemical pump is numerically simulated by the CFD software FLUENT. The result of calculation is compared with the result of PIV experiment, and the state of internal flow in chemical pump is elementary analyzed. The conclusions gained are listed as follows:

1. The internal flow which is simulated in impeller is coincide with the general rule of flow in the impeller machinery, and meanwhile it also basal inosculate with the result of PIV experiment
2. When the pump operation deviates from the design condition, outlet velocity of the impeller is different from the velocity in the extruding-room and the impaction will happen, which makes the calculation different from the practical situation.

3. With the process of the increasing flux and the decreasing pressure, the pressure between the vane's working face and back face changes differently and it decreases faster in back face than that in working face.
4. Because of the diffusion of impeller channel and the existence of secondary flow in the impeller, the boundary-layer separation happens and it also leads to the loss of separation.
5. The inlet setting angle can be designed as the fluid flow angle be plus with forward attack angle, which will enlarge the area of flow end plane, reduce the current velocity, relieve the crowding effect in the impeller and improve the pump's cavitation performance.
6. The analysis of numerical simulation and experiment with the medium of water in chemical pump, which will be helpful for the research of two-phase flow in the chemical pump.

Acknowledgements

The authors acknowledge the support received from "National Natural Science Foundation of China" (NO. 50476068) and " Key Lab Opening Fund of JiangSu" (NO. Cy0601).

References

1. Minguan, Y., Dong, L., Can, K. (2006). Analysis of flow with salt's separation and accumulation in centrifugal pump impeller. *Transactions of the Chinese Society of Agricultural Machinery*, 12, 83-86.
2. Kelder, J.D.H., Dijkers, R.J.H. & van Esch, B.P.M. (2001) .Experimental and theoretical study of the flow in the volute of a low specific-speed pump. *Fluid Dynamics Research*, 4, 267-280.
3. Mehta M., Kadambi, J.R. & Sastry, S. (2004). Study of particulate flow in the impeller of a slurry pump using PIV. *Proceedings of the ASME Heat Transfer/Fluids Engineering Summer Conference*. 489-499.
4. Sankovic, J.M.K. (2004). PIV investigations of the flow field in the volute of a rotary blood pump. *Journal of Fluids Engineering*, 5, 730-734.
5. Poroseva, S. & Iaccarino, G. (2001). Simulating separated flows using the k-ε model. *Center for Turbulence Research Annual Research Briefs*, 375-383.
6. Launder, B.E. and Spalding, D.B. (1974). The numerical computation of turbulent flows. *Computer Methods Appl. Mech. Eng.*, 3(4), 269-289.
7. Adrian, R.J. (1991). Particle-imaging techniques for experimental fluid mechanics. *Annual Review Fluid Mechanics*, 23(3), 261-306.
8. Fernandez, J. & Santo Laria, C. (2002). A numerical analysis of a mixed flow pump. *Proceeding of ASME FEDSM'02. ASME 2002 Fluids Engineering Division Summer Meeting*, 791-798 .